

SST Workshop, Tokyo, 3-5 December 2001

Laminar-turbulent transition prediction in supersonic flow : state-of-the-art at ONERA

D. Arnal

ONERA /DMAE

2 avenue Edouard Belin – 31055 Toulouse Cedex 4 – France

1- Introduction

The prediction of laminar-turbulent transition in boundary layers is one of the most important challenges for supersonic applications, because transition separates a laminar region with low skin friction from a turbulent region where skin friction dramatically increases. Therefore drag coefficient strongly depends on the boundary layer state.

It is established today that transition is triggered by the available disturbance environment: noise, free-stream turbulence, vibrations, surface polishing... Depending on the amplitude of these excitations, distinction is made between “natural” transition (low amplitude excitations) and “bypass” transition (high amplitude excitations). Paragraph 2 of this paper is devoted to an overview of the prediction methods used at ONERA in the case of “natural” transition. In paragraph 3, we consider a particular type of “bypass” transition, the so-called “leading edge contamination”, which plays a very important role for many practical applications.

2- “Natural” transition

The first stage of the transition process is the boundary layer receptivity [1]. Receptivity describes the means by which the forced disturbances enter the laminar boundary layer, as well as their signature in the disturbed flow. This signature constitutes the initial conditions for the development of boundary layer eigenmodes, which take the form of waves travelling in the downstream direction (these waves are referred to as the Tollmien-Schlichting (TS) waves for a two-dimensional, low speed flow without pressure gradient). In the second stage of the transition process, these waves exhibit a very small amplitude, so that their amplification or their damping can be described by the linear stability theory. When the amplitude of the waves reaches a finite amplitude, nonlinear phenomena take place and the breakdown to turbulence occurs a short distance downstream.

A rigorous prediction of transition location would require an accurate modeling of these three stages. For the sake of simplicity, the receptivity problem will not be considered here. Emphasis will be given on prediction methods based on linear theory (paragraph 2-1) and on weakly nonlinear theory (paragraph 2-2).

2-1- Linear stability theory and e^N method

Today, the linear stability theory is the only theoretical tool which can be used for practical transition predictions. It has been used for many years in its *local* formulation, the simplest expression of which is the well known Orr-Sommerfeld equation. More recently, a *nonlocal* formulation has been proposed in order to make the theory more rigorous and more general. Both approaches are discussed below.

2-1-1- Local approach

It is assumed that the small disturbances can be written as:

$$r' = r(y) \exp(\sigma x) \exp [i(\alpha x + \beta z - \omega t)] \quad (1)$$

r' denotes a velocity, pressure, density or temperature fluctuation. r is an amplitude function, which depends on y only (y is the distance normal to the wall), σ represents a spatial growth rate in the mean flow direction x , α and β are the components of the wave vector in the x and z directions, $\omega = 2\pi f$ is the wave frequency. $\psi = \tan^{-1}(\beta/\alpha)$ is the angle between the x direction and the wave vector.

The mean flow (U, V, W) is known. In the framework of the local theory, it is assumed that the mean flow is locally parallel, i.e. $V = 0$, $U = U(y)$, $W = W(y)$. As the disturbances are of infinitesimal amplitude, the quadratic terms are neglected. This leads to a system of ordinary differential equations in y for the amplitude functions $r(y)$. These equations are homogeneous with homogeneous boundary conditions, so that there exists a trivial solution $r(y) = 0 \quad \forall y$. In order to find “interesting” solutions, one has to solve an eigenvalue problem, i.e. to determine the combinations between α , β , σ and ω leading to non-trivial solutions.

In order to predict transition location, use is made of e^N method, see [2] for a complete overview. In the simple case of a two-dimensional, incompressible flow, it can be demonstrated that it is sufficient to consider waves with $\psi = 0$ or $\beta = 0$. For a fixed frequency $f = \omega/2\pi$, the spatial growth rate σ is integrated in the x direction. This gives:

$$\ln(A/A_0) = \int_{x_0}^x \sigma dx \quad (2)$$

where A is the wave amplitude at any abscissa and A_0 is the wave amplitude at the abscissa x_0 where it becomes unstable. After the total growth rate has been determined for all the unstable disturbances, it is easy to compute the N factor :

$$N = \underset{f}{\text{Max}} [\ln(A/A_0)] \quad (3)$$

The e^N method assumes that transition occurs for a predefined value of the N factor. In other words, the breakdown to turbulence is observed when the most amplified wave has been amplified by a critical ratio e^N . In free flight conditions, it is often assumed that the critical N factor lies in a range from 9 to 11.

The problem becomes more difficult for two-dimensional, compressible flows and for three-dimensional flows, because non-zero values of β (or ψ) need to be considered. There are several strategies allowing to take into account oblique waves.

The first possibility is to use the envelope strategy. At a given streamwise position x and for a fixed value of f , the growth rate σ is calculated as a function of ψ in order to determine the most unstable wavenumber direction, denoted as ψ_{\max} . The total growth rate and the N factor are then computed by replacing σ by $\sigma_{\max} = \sigma(\psi_{\max})$ in (2).

A second solution is the fixed β strategy. Here the total growth rate is integrated by following waves with constant values of f and β , and the final maximisation is done with respect to both parameters. Other strategies are available, see [2] for details.

Let us consider first applications of the e^N method for two-dimensional supersonic flows. In this case, the envelope strategy and the fixed β strategy provide similar results. A

limited amount of experimental data is available for free flight conditions at supersonic speed. For instance, transition measurements have been performed by Dougherty and Fisher [3] on a sharp cone fixed at the nose of a F-15 aircraft ; stability analyses indicated that the measured transition locations were rather well correlated with N factors around 10.

In most of the conventional wind tunnels, however, transition locations measured on simple models such as flat plates or cones at zero angle of attack correspond to significantly lower N factors, typically from 4 to 6. This is due to the fact that the turbulent boundary layer developing along the nozzle walls radiates pressure fluctuations (noise) which decrease the transition Reynolds numbers as compared with free flight conditions. To reduce the radiated noise in the ground facilities, it is necessary to keep the boundary layer in the laminar state along the nozzle walls. This has been done in the Mach 3.5 “quiet” tunnel at NASA Langley [4] by improving the flow quality in the settling chamber, by introducing a suction slot upstream of the throat as well as by a careful design and a high degree of polishing of the nozzle. This made it possible to closely simulate free flight conditions. Attempts to design “quiet” supersonic wind tunnels are in progress at Purdue University and at ONERA [5].

Before to present applications of the e^N method for three-dimensional flows, it is necessary to say a few words about the transition physics in such situations. A three-dimensional mean velocity profile can be decomposed into a streamwise component u in the free stream flow direction and a crossflow component w in the direction normal to the previous one. As the streamwise mean velocity profile looks like a classical two-dimensional profile, it generates unstable waves similar to the classical TS waves. The crossflow velocity profile exhibits an inflection point towards the boundary layer outer edge, so that its instability is of the inviscid type. The corresponding instability waves are named crossflow (CF) waves ; their frequency range is rather low ; in particular stationary disturbances ($f=0$ Hz) are highly unstable. CF instability is particularly powerful in accelerated flows, for instance near the attachment line of a swept wing.

Systematic applications of the e^N method in three-dimensional flows are currently carried out in the framework of an ONERA internal project on “Supersonic Aerodynamics”. For this purpose, experiments have been performed in the R1Ch wind tunnel at Mach 3 on a swept cylinder. Figure 1 shows a typical example of experimental results; the wall heat flux is plotted as a function of the azimuthal angle θ , $\theta=0^\circ$ corresponding to the attachment line. In the present case, transition is mainly triggered by CF disturbances. It occurs at $\theta \approx 35^\circ$, which corresponds to a N factor around 20. On the other side, experiments performed in the same wind tunnel on a flat plate gave transition N factors around 4.

These results seem to indicate that it is necessary to consider two different N factors, one for TS instability (N_{TS}) and another for CF instability (N_{CF}), with $N_{CF} > N_{TS}$. A possible explanation is that both kinds of waves are not generated by the same receptivity mechanisms. TS waves are generated by free stream disturbances (noise), whereas CF waves are less sensitive to the disturbance environment. In particular low speed experiments by Saric et al [6] demonstrated that surface polishing is the main parameter governing the initial amplitude of CF instabilities. If this result is still valid for high speed flows, then “quiet” tunnels would not be necessary for investigating CF instability. Experiments by King at Mach 3.5 seem to support this assumption [7].

Other linear stability computations have been performed in the framework of a NAL-ONERA cooperation dealing with natural laminar flow control on a NAL model tested at ONERA Modane (NEXST-1 airplane project). The results are discussed in a joint NAL-ONERA paper presented in this workshop.

2-1-2- Nonlocal approach

In the last years, the linear theory has been extended in order to take into account non parallel effects. The new expression of the disturbances is:

$$r' = r(x, y) \exp\left(\int \sigma(\xi) d\xi\right) \exp\left[i\left(\int \alpha(\xi) d\xi + \beta z - \omega t\right)\right] \quad (4)$$

where β is constant. In contrast to the usual, local approach, the amplitude functions depend on x and y , and the parameters σ et α depend on x . Substituting expression (4) into the stability equations, neglecting $\partial^2 r / \partial x^2$ as well as the quadratic terms yield a system of partial differential equations which are parabolic in the x direction ; these equations are often referred to as Parabolized Stability Equations (PSE), see [8] for details. They are solved using a marching procedure in x with prescribed initial conditions. As the results at a given streamwise position depend on the upstream history of the disturbances, this approach is called nonlocal.

It is of course possible to use the nonlocal approach for calculating a “nonlocal N factor”. As β is constant in (4), the only possible integration strategy is the fixed β strategy. Systematic comparisons between local and nonlocal N factors, for subsonic and supersonic flows, led to the following conclusions:

- the computing time for both approaches is similar;
- the nonparallel effects are destabilizing, i.e. nonlocal growth rates are larger than local growth rates in the regions where the boundary layer thickness increases rapidly;
- even if the nonlocal theory is more rigorous than the local one, there is no reduction in the scatter of the N factor at transition.

The last sentence implies that the nonlocal approach does not improve the accuracy of boundary layer transition prediction. In fact, the main interest of the nonlocal computations is to provide initial conditions for nonlinear computations as described below.

2-2- Weakly nonlinear theory

The disturbances are now written as double Fourier expansions containing two- and three-dimensional discrete normal modes denoted as (n, m) modes:

$$r'_{nm} = r_{nm}(x, y) \exp\left(\int \sigma_{nm}(\xi) d\xi\right) \exp\left[i\left(\int \alpha_{nm}(\xi) d\xi + m\beta z - n\omega t\right)\right] \quad (5)$$

It can be seen that n represents the time dependence, and m the spanwise dependence. As it has been done in the linear PSE approach, the x -dependence of the (n, m) modes is shared between the amplitude functions and the exponential terms. Introducing a truncated form of (5) into the Navier-Stokes equations leads to a system of coupled partial differential equations (nonlinear PSE) which is solved by a marching procedure [8].

It is obvious that the nonlinear theory is more complicated to use than the linear theory. In any case, linear computations are first performed in order to determine the most unstable frequencies and their spanwise wavenumber β . Initial conditions for the nonlinear computations must be prescribed at a given initial location x_0 . In general, two or three major (n, m) modes are selected with prescribed initial amplitudes, and the amplitudes of the other (minor) modes is calculated by solving approximate equations. Then the nonlinear computation proceeds downstream. The objective is to obtain “something interesting” at the measured or prescribed transition location. “Something interesting” means a strong nonlinear interaction between modes which were travelling independently of each other in the upstream

linear region. Therefore nonlinear results will depend on two choices: the choice of a relevant interaction scenario and the choice of the initial amplitudes of the major modes.

Many nonlinear computations have been performed at ONERA in subsonic and transonic flows, for two- and three-dimensional problems. The most interesting TS-TS, TS-CF and CF-CF interaction scenarios have been identified, and “standard” initial amplitudes have been determined, see [9]. However, nonlinear results for supersonic flows are rather scarce. Figure 2 shows results for a two-dimensional flat plate at Mach 3. The logarithm of the amplitude of some modes is plotted as a function of x . The full lines correspond to linear results and the symbols correspond to the nonlinear results. The chosen major modes are the (1,1) and the (1,-1) modes, with $f = 20$ kHz and $\beta = 750$ ms⁻¹. These modes represent two oblique waves propagating with wavenumber angles equal to ψ and $-\psi$. For symmetry reasons, the amplitudes of both modes are identical. It can be seen that the initially minor (0,2) mode first follows the linear evolution, then its amplitude increases very rapidly, indicating a strong nonlinear interaction for $x > 0.1$ m. The (0,0) mode associated with a mean flow distortion is also growing, whereas it is highly stable in the framework of the linear theory. The computation breaks down at $x \approx 0.28$ m. At this point, all the considered modes reach a large amplitude (between 1 and 10 percent of the free stream velocity). This can be considered as the beginning of laminar-turbulent transition.

This example demonstrates that nonlinear PSE are useful for the understanding of transition phenomena, but there is no proof that the transition scenario investigated in figure 2 (the so-called “wave-vortex triad”) is the most efficient. In addition, other initial amplitudes would result in a “numerical breakdown” taking place at different locations. Therefore an extensive numerical data base needs to be established before the nonlinear theory can be used with confidence for transition prediction.

3- “Bypass” transition

Another route to turbulence is the so-called « bypass » mechanism which is observed in the presence of high amplitude environmental disturbances. A typical example is the contamination of a swept wing attachment line by turbulent structures. In this case, linear theory non longer applies and simple, purely empirical criteria should be used.

3-1- Leading edge contamination criterion

The attachment line represents a particular streamline which divides the flow into one branch following the upper surface and another branch following the lower surface. For low speed flows, the boundary layer flow along the attachment line is usually characterised by the Reynolds number \bar{R} defined as:

$$\bar{R} = \frac{W_e \eta}{\nu_e} \quad \text{with} \quad \eta = (\nu_e / k)^{1/2} \quad (6)$$

W_e is the free stream velocity component parallel to the leading edge, ν_e is the kinematic viscosity, and k is the free-stream velocity gradient around the attachment line.

Leading edge contamination is likely to occur when a swept body is attached to a solid surface (fuselage, wind tunnel wall...). This problem has been widely studied for low speed flows and a simple criterion based on the value of \bar{R} was developed (see Pfenninger [10], Poll [11]). If \bar{R} is lower than 250, the turbulent bursts convected along the wall are damped and vanish as they travel along the attachment line. However, for $\bar{R} > 250$, these bursts are self-sustaining. They grow, overlap and the leading edge region becomes fully turbulent.

Poll extended this simple criterion to supersonic and hypersonic flows by introducing a modified length scale η^* and a modified Reynolds number \bar{R}^* which have the same definition as η and \bar{R} , except that ν_e is replaced by ν^* . The latter quantity is the kinematic viscosity computed at a reference temperature T^* which may be estimated from an empirical relationship [12].

3-2- Validation of the leading edge contamination criterion

Two series of experiments have been performed at ONERA in order to investigate leading edge flows on swept models in supersonic flow. The first objective was to assess the criterion proposed by Poll for leading edge contamination. A complete description of these experiments can be found in [13].

The first experiment was carried out on a cylinder placed with a sweep angle in the jet exhaust of the supersonic R1 Chalais-Meudon (R1Ch) wind tunnel. A flat plate generates a turbulent boundary layer at the attachment line of the cylinder. The flat plate is placed at zero angle of attack with respect to the incoming flow direction. The tests were carried out at Mach 3 for two sweep angles of the cylinder (20° and 30°). The cylinder is equipped with pressure taps and thermocouples from which the state of the boundary layer can be determined through the value of the Stanton number. Figure 3 shows a diagram with the evolution of the Stanton number versus \bar{R}^* . Laminar and turbulent theoretical boundaries are indicated on this diagram. The measured Stanton number begins to deviate from the laminar law for $\bar{R}^* \approx 200$ and the fully turbulent regime is reached for $\bar{R}^* \approx 260$. These results are not in contradiction with Poll's criterion.

This value has also been confirmed by another experiment on a swept wing whose leading edge was designed to provide in the wind tunnel conditions \bar{R}^* values close to the flight values. The wing was tested in the supersonic S5 Chalais-Meudon (S5Ch) wind tunnel for Mach numbers 2 and 2.5 at a sweep angle of 74°. It was fixed to the wind tunnel upper wall, and the boundary layer was turbulent at the wall-wing junction. Pressure distribution around the leading edge and wall temperature measurements allowed to compute \bar{R}^* . The state of the boundary layer was determined through hot films signals as shown in figure 4. For \bar{R}^* values < 200 the signals indicate a laminar boundary layer. For $\bar{R}^* \approx 200$ turbulent spots appear and for $\bar{R}^* > 250$ the signals show that the boundary layer is turbulent.

It is interesting to notice that the results obtained in both series of experiments are close together, although the test conditions are completely different. In particular, the leading edge was subsonic in the S5Ch experiments and supersonic (bow shock) in the R1Ch experiments. This demonstrates that \bar{R}^* is the significant parameter which governs leading edge contamination in supersonic flow.

4- Conclusion

Today, the linear stability theory associated with the e^N method remains the only practical tool for transition prediction. Comparison between local and nonlocal results shows that taking into account the nonparallel effects does not improve the accuracy of the method; in all cases, the key problem lies in a judicious choice of the N factor at transition. Further experiments are needed in order to confirm the fact that there are in general two N factors for TS and for CF dominated transition processes.

The weakly nonlinear theory is not (yet) a practical tool for transition prediction. Systematic computations need to be performed in order to constitute a numerical database collecting the most interesting interaction scenarios and “standard” initial amplitudes. This is particularly necessary for supersonic flows for which the amount of numerical results is still limited. On the other side, nonlinear PSE present an unquestionable interest for the understanding of the transition phenomena.

As far as the problem of leading edge contamination is concerned, the two series of experiments reported in this paper demonstrated that the first turbulent spots appear for $\bar{R}^* \approx 200$ and that the attachment line is fully turbulent for $\bar{R}^* \approx 250$. Therefore the critical value proposed by Poll seems to be close to the limit corresponding to the completion of leading edge contamination.

In real flight conditions, the values of \bar{R}^* on aircraft wings are usually much larger than the critical value 250, at least near the root [13]. However, in order to apply Laminar Flow Control, the attachment line on the wing has to be laminar. Several solutions have been successfully tested for transonic swept wings at ONERA [14] but the experience is very limited for supersonic wings. The efficiency of suction for increasing the contamination threshold will be investigated in the next step of this study.

Acknowledgments

We wish to thank our colleagues J.P. Archambaud, G. Casalis, F. Louis, J. Reneaux and A. Séraudie who performed the experiments or computations reported in this paper. The leading edge contamination experiments have been supported by the “Service des Programmes Aéronautiques” (SPAé).

References

- [1] Morkovin M.V. *Critical evaluation of transition from laminar to turbulent shear layers with emphasis on hypersonically travelling bodies*. Report AFFDL-TR-68-149, Wright-Patterson Air Force Base, Ohio, 1968
- [2] Arnal D. *Laminar-turbulent transition: prediction based on linear theory*. In Progress in transition modelling, AGARD Report No 793, 1993
- [3] Fisher D., Dougherty N. *In-flight transition measurements on a 10 deg. cone at Mach numbers from 0.5 to 2*. TP 1971. NASA, 1982
- [4] Beckwith I.E., Creel Jr T.R., Chen F.J., Kendall J.M. *Freestream noise and transition measurements on a cone in a Mach 3.5 Pilot low-disturbance tunnel*. TP 2180, NASA, 1983
- [5] Thibert J.J., Arnal D. *A review of ONERA aerodynamic research in support of a future supersonic transport aircraft*. Progress in Aerospace Sciences 36, pp. 581-627, 2000
- [6] Radetsky R.H., Reibert M.S., Saric W.S., Takagi S. *Effect of micron-sized roughness on transition in swept wing flows*. AIAA Paper 93-0076, 1993
- [7] King R. *Mach 3.5 boundary layer transition on a cone at angle of attack*. AIAA Paper 91-1804, 1991
- [8] Herbert T. *Parabolized Stability Equations*. In Progress in transition modelling, AGARD Report No 793, 1993

[9] Arnal D., Casalis G. *Laminar-turbulent transition prediction in three-dimensional flows*, Progress in Aerospace Sciences 36, pp. 173-191, 2000

[10] Pfenninger W. *Flow phenomena at the leading edge of swept wings*. AGARDograph 97, Part 4, 1965

[11] Poll D.I.A. *Some aspects of the flow near a swept attachment line with particular reference to boundary layer transition*. Technical Report 7805/K, Cranfield, College of Aeronautics, August 1978

[12] Poll D.I.A. *Boundary layer transition on the windward face of space shuttle during reentry*. AIAA Paper 85-0899, 1985

[13] Arnal D., Reneaux J. *Attachment line transition in supersonic flow*, in Aerodynamic Drag Reduction Technologies, Notes on Numerical Fluid Mechanics, Springer Verlag, 2001

[14] Reneaux J., Preist J., Juillen J.C., Arnal D. *Control of attachment line contamination*. 2nd European Forum on Laminar Flow Technology, Bordeaux (France), June 10-12, 1996 - ONERA TP 1996-84.

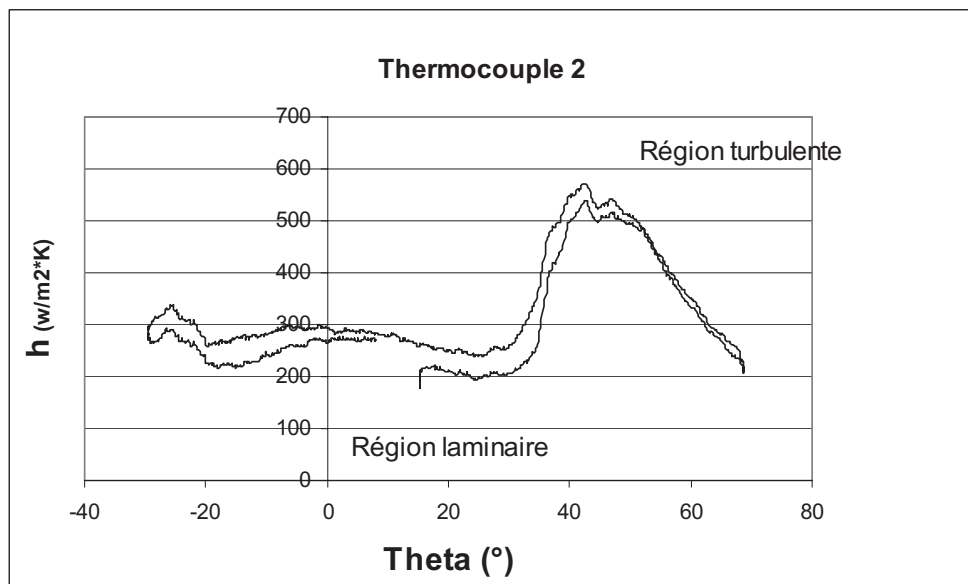


Figure 1- Wall heat flux measurement on a swept cylinder at Mach 3
(sweep angle = 40°, $P_i = 4.5$ bar, $T_i = 350$ K)

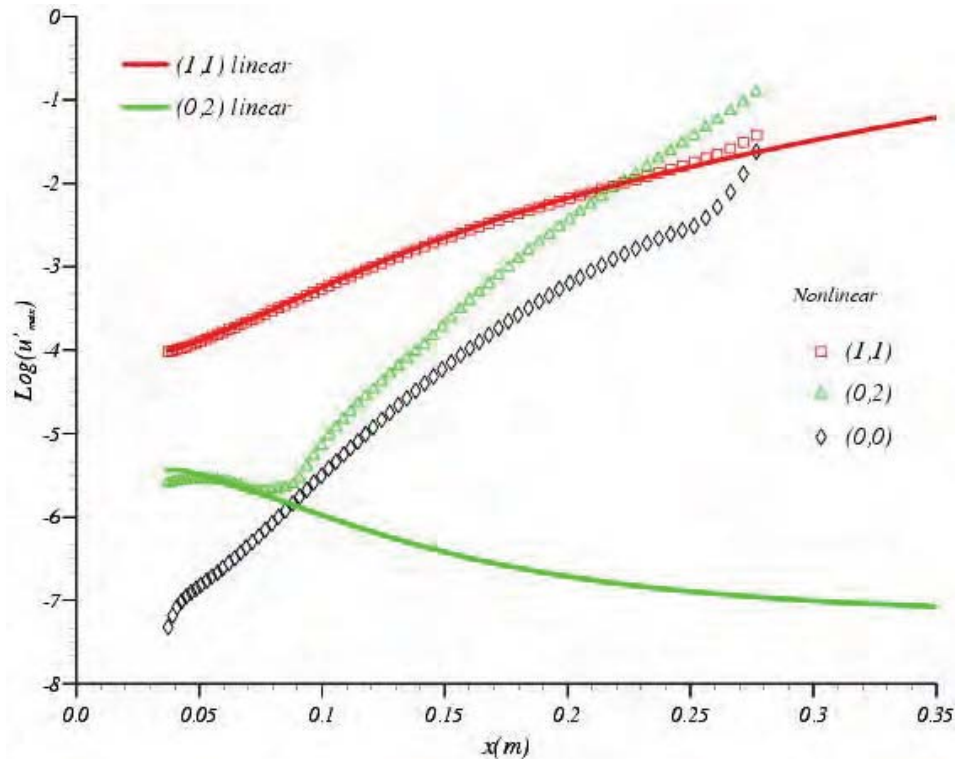


Figure 2- Nonlinear stability computations for a flat plate at Mach 3
($T_i = 324$ K, $P_i = 2.3$ bar)

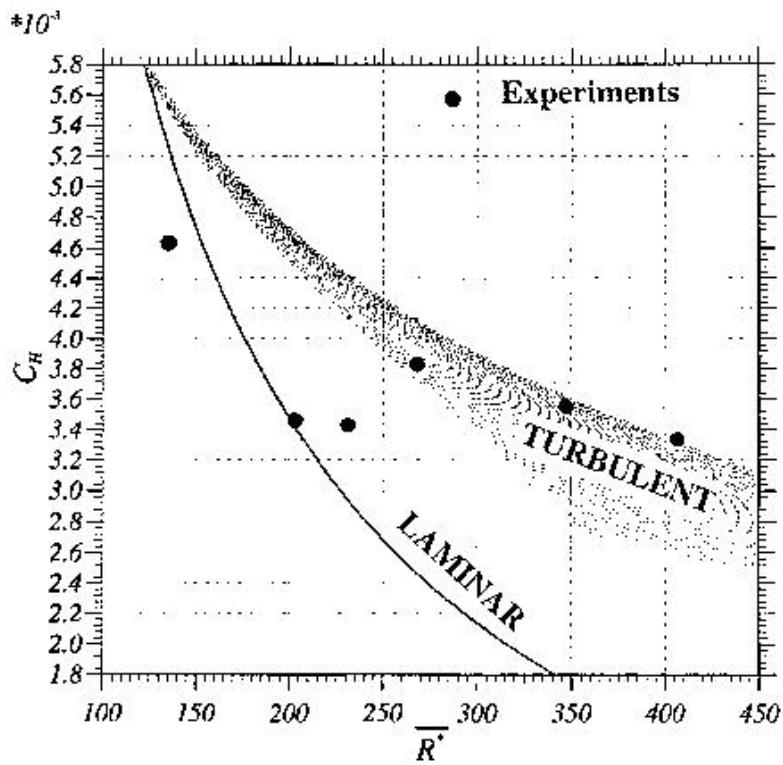


Figure 3- Example of experimental results (R1Ch wind tunnel)

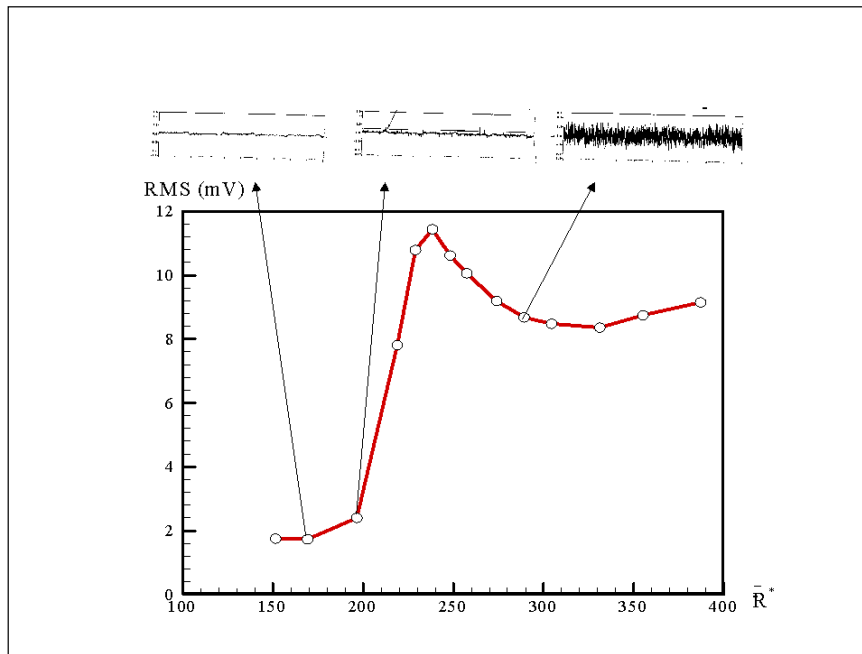


Figure 4- Example of experimental results (S5Ch wind tunnel)